Available online at www.sciencedirect.com
ScienceDirect
Chemical Physics 329 (2006) 139–147
Chemical Physics
www.elsevier.com/locate/chemphys

Cleavage of thymine N_3–H bonds by low-energy electrons attached to base π^* orbitals

Magali Théodore [1], Monika Sobczyk, Jack Simons *

Chemistry Department and Henry Eyring Center for Theoretical Chemistry, University of Utah, Salt Lake City, UT 84112, USA

Received 9 April 2006; accepted 8 May 2006
Available online 7 July 2006

Abstract

In this work, we extend our earlier studies on single strand break (SSB) formation in DNA to consider the possibility of cleaving a thymine N_3–H bond to generate a nitrogen-centered anion and a hydrogen radical which might proceed to induce further bond cleavages. In earlier studies, we considered SSBs induced by low-energy electrons that attach to DNA bases' π^* orbitals or to phosphate P=O π^* orbitals to cleave sugar–phosphate C–O bonds or base–sugar N_1–C bonds. We also studied the effects of base π-stacking on the rates of such bond cleavages. To date, our results suggest that sugar–phosphate C–O bonds have the lowest barriers to cleavage, that attachment of electrons with energies below 2 eV most likely occurs at the base π^* orbitals, that electrons with energy above 2 eV can also attach to phosphate P=O π^* orbitals, and that base π stacking has a modest but slowing effect on the rates of SSB formation. However, we had not yet examined the possibility that base N_3–H bonds could rupture subsequent to base π^* orbital capture. In the present work, the latter possibility is considered and it is found that the barrier to cleavage of the N_3–H bond in thymine is considerably higher than for cleaving sugar–phosphate C–O bonds, so our prediction that SSB formation is dominated by C–O bond cleavage remains intact.

Keywords: Thymine; DNA damage; Shape resonance; Metastable anion

1. Introduction

There has been considerable recent interest [1] in the fact that low-energy electrons (i.e., electrons with kinetic energies below ionization or electronic excitation thresholds of DNA or of water) have been observed to damage DNA and in the mechanisms by which this can occur. This group's involvement in the study of how low-energy electrons may damage DNA was nurtured by experiments from Boudaiffa et al. [2] who observed single strand breaks (SSBs) to occur in relatively dry samples of DNA [3] when free electrons having kinetic energies as low as 3.5 eV were used. The existence of peaks in the plots of SSB yield vs. electron kinetic energy, combined with earlier knowledge from the Burrow group of the energies [4] at which DNA's four bases' π^* orbitals attach electrons, lead the authors of Ref. [2] to suggest that the SSBs likely occur by formation of a metastable resonance anion state. Because the SSB peaks occurred at energies (>3.5 eV) considerably above the lowest base π^* anion-state energies of the bases, the authors of Ref. [2] suggested that core-excited resonances are likely involved in which one attaches an electron to a π^* orbital and simultaneously excites another electron from a π to a π^* orbital.

Subsequent to the experimental findings of Ref. [2] we carried out a series of theoretical simulations aimed at:

1. considering electron attachment to base π^* or phosphate P=O π^* orbitals,
2. considering cleavage of a variety of bonds that could lead to SSB formation and that would be expected to have low barriers to cleavage because they produce very stable anionic fragments,

* Corresponding author.
E-mail address: simons@chemistry.utah.edu (J. Simons).
[1] Also Computational Chemistry Group, Physical and Chemical Properties, Division, National Institute of Standards and Technology, Gaithersburg, MD 20899-8380, USA.

0301-0104/$ - see front matter © 2006 Elsevier B.V. All rights reserved.
doi:10.1016/j.chemphys.2006.05.012

3. predicting the rates of such bond cleavages and thus determining which bond(s) are most likely to be involved in SSB formation.

After our making predictions that even lower-energy electrons than studied in Ref. [2] could attach to DNA and cause SSBs and that it is the sugar–phosphate C–O bonds that are most susceptible to such cleavage, two important experimental verifications appeared. In one, the Sanche and Burrow groups [5] collaborated and studied electrons in the range (0–4 eV) where we predicted shape resonances could induce stand breaks and again observed SSBs at approximately the same yield as they found in the earlier work using electrons with >3.5 eV energy. Moreover, they showed that the shape of the SSB yield vs. electron energy plot could be duplicated by superposing the shapes of the electron attachment vs. electron energy plots of the four DNA bases. In the second [6] publication, the Sanche group carried out chemical analysis of the fragments formed upon electron-induced bond cleavage of DNA base oligomers and found that indeed sugar–phosphate C–O bond cleavage is the dominant fragmentation path leading to SSB formation under these conditions.

We therefore feel confident that our approach to studying bond cleavages in DNA induced by the attachment of low-energy electrons is methodolically sound and is providing important new insights. In this paper, we extend these studies to include consideration of base N_3–H bond rupture which, by itself, would not produce a rupture in the DNA's backbone structure but which could if the hydrogen atom thus released subsequently attacked the sugar or phosphate units. In Section 2 of the present paper, we review our findings to date on these matters as well as what has been found experimentally subsequent to our investigations. Section 3 describes the methods we use, Section 4 contains the results of our current study, and in Section 5 we summarize our findings.

2. Review of our earlier studies

As discussed above, early solid experimental data showed that electrons with energies >3.5 eV could attach to DNA and induce SSBs. However, which bonds are broken in the SSBs and the details of the mechanism of bond rupture were not yet resolved nor was the possibility of attachment to base π^* orbitals or to other orbital sites firmly established. We therefore undertook several theoretical studies [7–11] in which we excised [12] one or three base–sugar–phosphate units (an example is shown in Fig. 1) of DNA or a sugar–phosphate–sugar unit and used theoretical simulations to further probe these matters.

The model systems treated in Refs. [7–11] consisted of a cytosine- or thymine-containing fragment linked to a sugar and a phosphate, three such cytosine-containing fragments linked by phosphate groups and π-stacked, and a sugar–phosphate–sugar unit.

2.1. Cytosine or thymine electron attachment

The primary findings of two of our earlier studies are summarized below in Fig. 2, Tables 1 and 2. In Fig. 2, we plot the energy of the cytosine–sugar–phosphate fragment as the phosphate–sugar O–C bond is stretched [13] both in the absence of the attached electron and with an electron attached to cytosine's lowest π^* orbital. We plot these data both for an isolated (i.e., non-solvated) fragment as is representative of the samples in [2] and when solvated by a medium characterized by a dielectric constant ε of 78. We performed the solvated-fragment

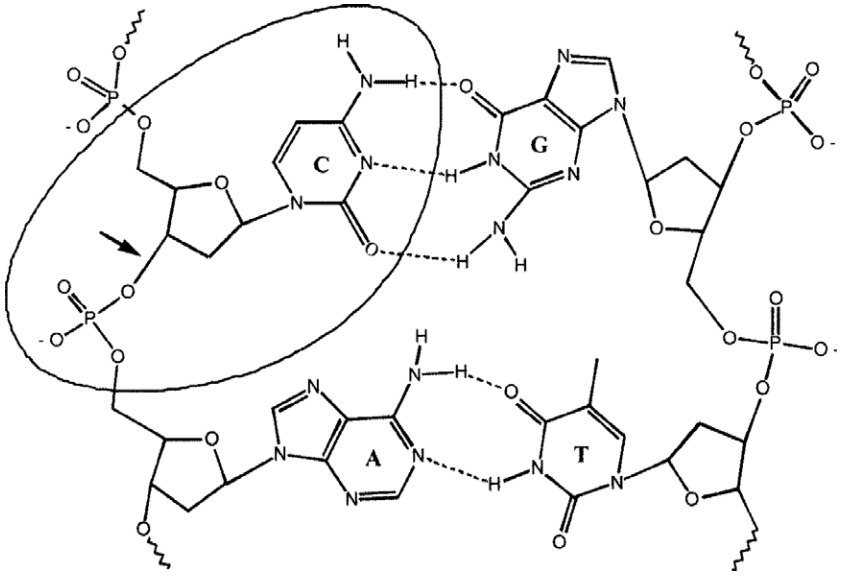

Fig. 1. Fragment of DNA excised for study in Refs. [7,8] showing the cytosine–sugar–phosphate fragment and the bond that rupture (in Ref. [9] the fragment of DNA studied contains thymine instead of cytosine) (taken from Ref. [7]).

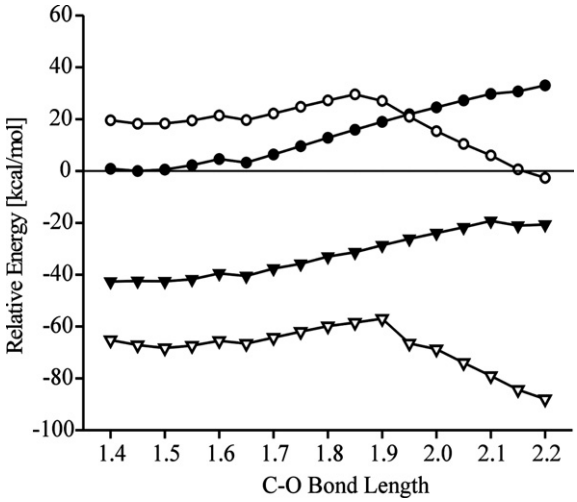

Fig. 2. Energies of neutral (filled symbols) and anionic (open symbols) cytosine-containing DNA fragment vs. C–O bond length (Å) as isolated species (top two plots) and with $\varepsilon = 78$ (bottom two plots) (taken from Ref. [8]).

Table 1
Barriers (kcal/mol) along the C–O bond length for various electron kinetic energies E (eV) and various solvent dielectric constants ε for the cytosine–sugar–phosphate fragment (from Ref. [8])

Electron energy E (eV)	0.2	0.3	0.8	1.0	1.3	1.5
Barrier ($\varepsilon = 1.0$)	16	15	12	11	9	8
Barrier ($\varepsilon = 4.9$)	18	18	13	10	10	8
Barrier ($\varepsilon = 10.4$)	19	20	14	10	10	8
Barrier ($\varepsilon = 78$)	28	22	11	9	5	5

Table 2
Barriers (kcal/mol) along the C–O bond length for various electron kinetic energies E (eV) and various solvent dielectric constants ε for the thymine–sugar–phosphate fragment (from Ref. [9])

Electron energy E (eV)	0.25	0.3	0.45	1.0
Barrier ($\varepsilon = 1.0$)	13	13	10	8
Barrier ($\varepsilon = 4.9$)	17	15	14	10
Barrier ($\varepsilon = 10.4$)	18	17	14	11
Barrier ($\varepsilon = 78$)	25	19	15	7

simulations to gain some idea of how large an effect solvation might have on the SSB formation process we were considering.

Three crucial observations to make from Fig. 2 are:

(1) that the anion surface has a barrier near $R = 1.9$ Å and subsequently drops to lower energy as R is further increased, while the neutral-fragment surface monotonically increases with R indicative of homolytic cleavage of the C–O bond,
(2) that the anion is electronically metastable with respect to electron autodetachment when solvation is absent but can be rendered electronically stable if solvation is sufficient,
(3) that even strong ($\varepsilon = 78$) solvation does not alter the height or location of the barrier on the anion surface very much.

Analogous curves were obtained for the thymine–sugar–phosphate unit of Ref. [9]. The heights of the barriers on the cytosine and thymine electron-attached curves are the most important ingredients in determining the sugar–phosphate C–O bond cleavage rates. These barrier heights were computed for a range of solvation strengths and for a range of electron kinetic energies for the cytosine- and thymine-containing fragments and the results are summarized in Tables 1 and 2.

The range of electron energies E is representative of the range spanned by the low-lying π^* orbitals of cytosine and thymine. The trends in the data on the cytosine-containing DNA fragment (Table 1) are qualitatively the same as those we obtained for a thymine-containing species (Table 2), although there are quantitative differences in the bond-cleavage rates and in how these rates depend on electron energy E and solvation strength ε.

From the above barrier data, we were able to estimate the rates of C–O bond breakage subsequent to electron attachment by multiplying the frequency at which a typical C–O bond vibrates (ca. 10^{13} s^{-1}) by the probability P that thermal motions can access the barrier height Δ: $P = q^{-1}\exp(-\Delta/kT)$ where q is the vibrational partition function for the N_3–H vibration. We found these barriers Δ to vary from ca. 5 to 28 kcal/mol for the cytosine-containing fragment (Table 1) and from 7 to 25 kcal/mol for the thymine-containing (Table 2) fragment; they are smallest at higher E-values and they depend on the solvation environment as shown in Tables 1 and 2.

It was thus suggested in Refs. [7–11] that accessing the barrier on the π^* anion surface would be the rate-limiting step in SSB formation (subsequent to electron capture) by the π^* base anion mechanism that we suggested. Further, it was predicted that C–O rupture rates as high as 10^{10} s^{-1} would occur.

2.2. Phosphate group attachment

In addition to identifying the barriers to C–O bond rupture for cytosine- and thymine-containing fragments when an electron is attached to a base π^* orbital, we also considered the fate of electrons that might attach directly to a (neutralized) phosphate fragment. Other workers had proposed [14] that rather than attaching to a DNA base π^* orbital as we had suggested [7–11], it may be possible for a very-low-energy electron to attach directly to a P=O π^* orbital of the phosphate moiety to form a P$^{\cdot}$–O$^-$ radical anion which might live long enough to subsequently induce rupture of a 3′ or 5′C–O σ bond. We improved on Ref. [14] by employing the so-called stabilization method [15,16] to obtain the resonance-state energies for the π^* state and the σ^* state in the region where these states are not stable [10]. In Fig. 3, we show the neutral and π^*- and σ^*-attached anion curves obtained using the stabilization method for fragmentation of the 3′C–O and 5′C–O bonds, respectively.

Our findings led us to conclude that:

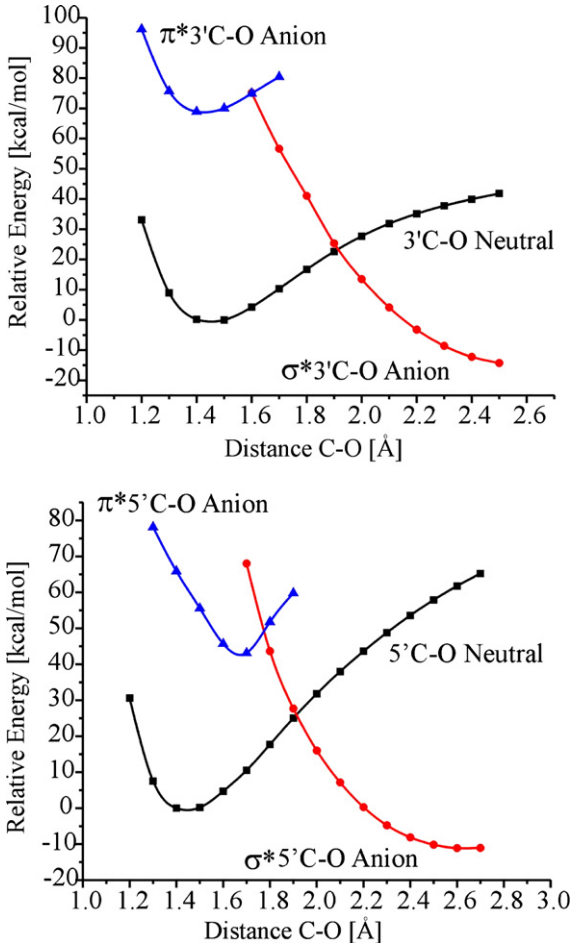

Fig. 3. Energies of neutral, π^* anion, and σ^* anion for 3′C–O (top) and 5′C–O (bottom) bond rupture vs. C–O bond length (taken from Ref. [10]).

(1) Unlike what was suggested in Ref. [14], electrons having kinetic energies near 0 eV cannot attach directly at significant rates to DNA's phosphate units (even if these units are rendered neutral by counter-ions).
(2) Electrons with energies in the 2–3 eV range (see Fig. 3) can attach directly (vertically) to DNA's (neutralized) phosphate group's P═O π^* orbital and form a metastable π^* anion which, by coupling to the repulsive O–C σ^* anion state, can lead to C–O bond cleavage.

Thus, we concluded that such anions can induce phosphate–sugar O–C σ bond cleavages but only at rates that we estimated (from the height of the barrier on the π^*/σ^* surface) to be ca. $10^6\ s^{-1}$ and only for electrons having energies in excess of 2 eV.

2.3. Effects of base π-stacking

We also examined the barriers to sugar–phosphate C–O bond cleavage for the π-stacked model compound shown in Fig. 4.

In Fig. 5, we show plots of the electronic energies of the neutral and base π^*-attached species for the energy E of the attached electron ranging from 0.3 to 2.0 eV. The π^*-anion

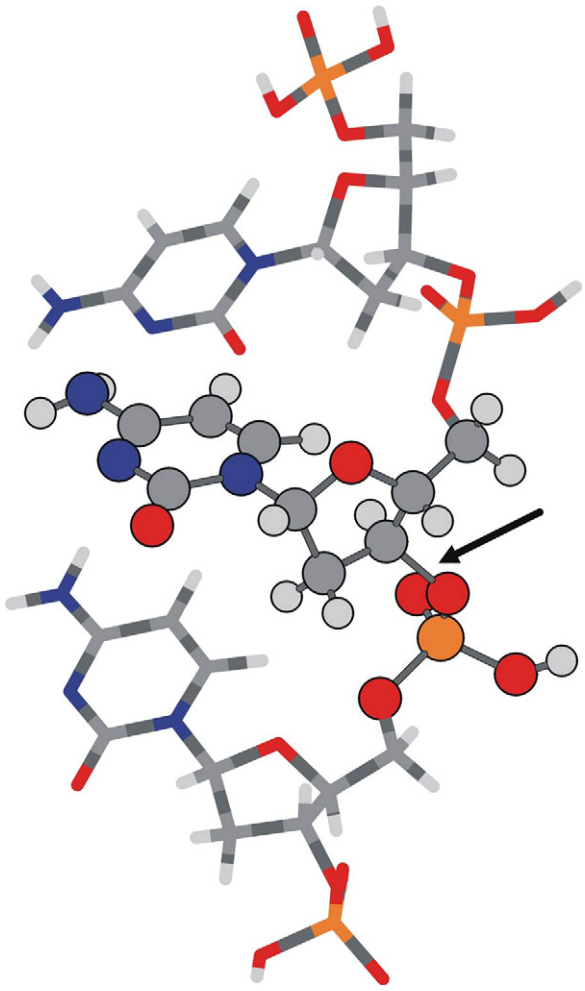

Fig. 4. Fragment of DNA showing the three nucleotides containing cytosine–sugar–phosphate units. The C–O bond cleaved in SSB formation is marked with an arrow (taken from Ref. [11]).

energy profiles suggest that C–O bond rupture requires surmounting a 11–25 kcal/mol barrier (depending on the electron energy E) but that the fragmentation process is exothermic in all cases. In Table 3, we collect from Fig. 5 values of the barrier heights along the C–O bond length for various E values, and we show the value of R at which the barrier occurs in each case.

Comparing the barrier heights for the single-cytosine–sugar–phosphate unit (Table 1) with those obtained for the fragment containing three nucleotides (Table 3), we note that π-stacking seems to increase the barrier heights [17] by ca. 8 kcal/mol. As a result, π-stacking can be expected to substantially lower the predicted rates of SSB formation compared to our predictions in [7–10].

2.4. Sugar–base C–N_1 bond cleavage

We also examined the possibility of breaking a sugar–cytosine C–N_1 bond. Although this would not cleave the backbone of DNA, it would lead to base release and the carbon-centered sugar radical formed could react with nearby groups to cause a strand break. As our earlier studies made

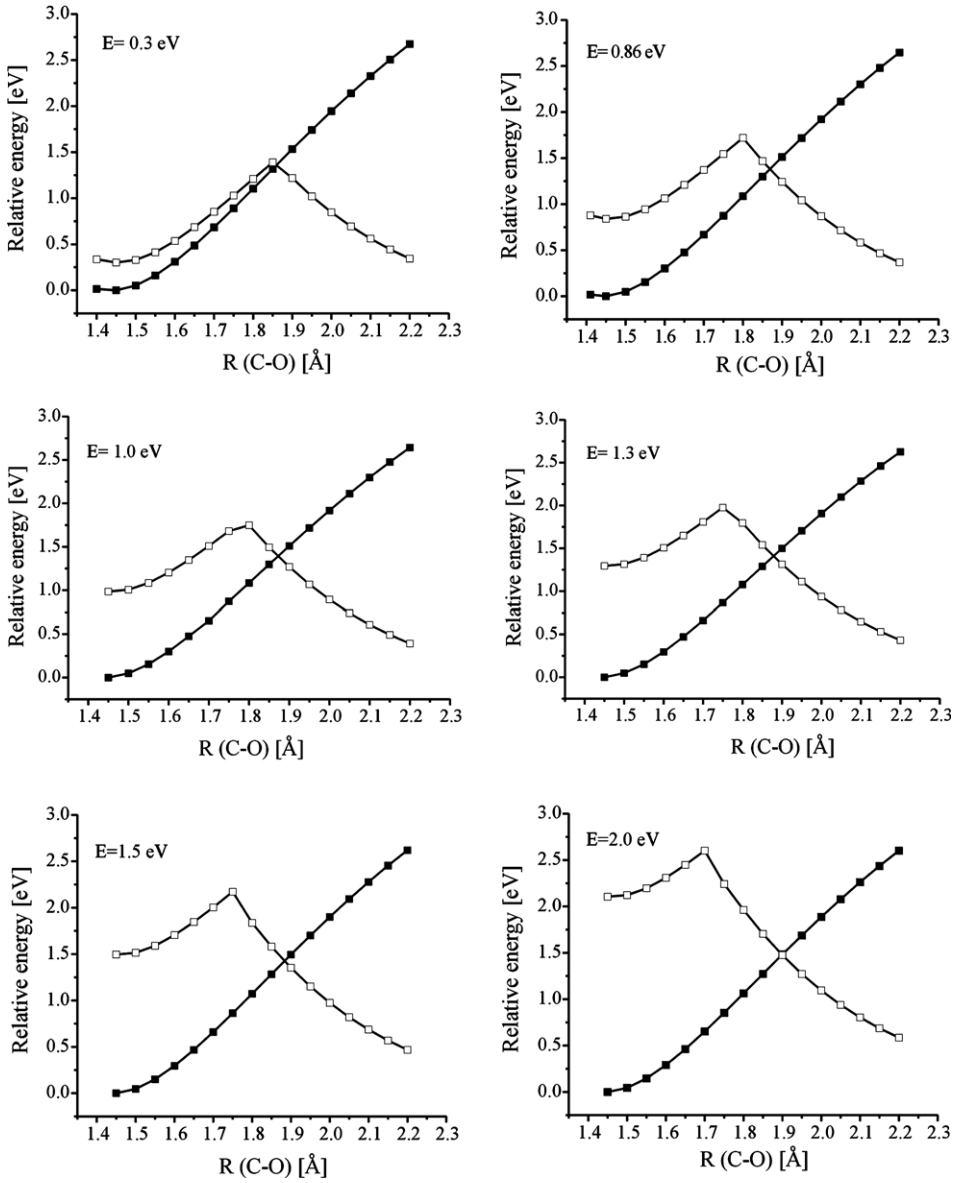

Fig. 5. Energies of neutral fragment (solid square symbols) and of the π^*-anion (open square symbols) fragment at various electron energies E (taken from Ref. [11]).

Table 3
Barriers (kcal/mol) and C–O bond lengths R (Å) at the barrier for various electron energies E (eV) for the three-nucleotide system

Electron energy E	0.3	0.86	1.0	1.3	1.5	2.0
Barrier	25	20	18	16	15	11
R at barrier	1.85	1.80	1.80	1.75	1.75	1.70

clear, it is the electronic stability of the anion formed when bond cleavage occurs that provides the thermodynamic driving force (and thus the low barriers on the anion surfaces) for bond breaking. We thought that the anion formed when a sugar–cytosine C–N_1 bond breaks could be stable enough to make this bond cleavage also facile, so we decided to address this issue.

In Fig. 6, we plot the energy of the cytosine–sugar–phosphate fragment as the sugar–cytosine C–N_1 bond is stretched both for the neutral and π^*-anion species for an electron energy of $E = 0.8$ eV (this energy was found to be in the range of the cytosine π^* orbitals as discussed earlier).

The π^*-anion energy profile suggests that C–N bond rupture requires surmounting a 43 kcal/mol barrier. Recall, that the barrier height calculated for the same energy of the attached electron ($E = 0.8$ eV) for C–O bond cleavage in cytosine–sugar–phosphate is 12 kcal/mol. Thus, we concluded that it is unlikely that SSB's can occur via sugar–cytosine C–N bond rupture at a rate that would compete with sugar–phosphate C–O bond rupture.

In Fig. 7, we summarize the bond-cleavage barrier data we obtained (illustrating, for example, the barriers when 1 eV electrons attach) for sugar–phosphate C–O, base–sugar N–C, and base N–H bonds.

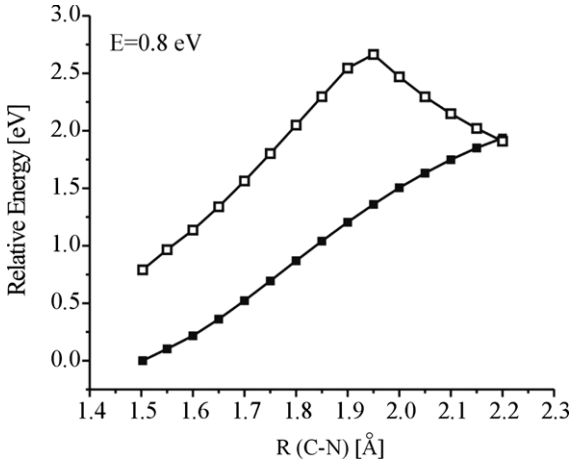

Fig. 6. Energies of the neutral (solid square symbols) and of the π^*-anion (open square symbols) DNA fragment vs. C–N bond length (Å) as isolated species at electron energy $E = 0.8$ eV (taken from Ref. [11]).

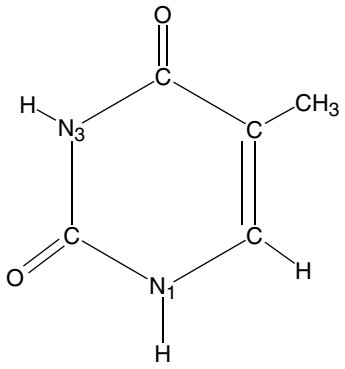

Fig. 8. The thymine molecule showing the N_3–H bond whose cleavage is studied here.

3. Methods

In this study, we consider cleavage of the N_3–H bond of an isolated thymine molecule as drawn in Fig. 8.

We chose this fragment to examine partly because of recent elegant experimental results [18] showing the H atom loss from thymine occurs for electrons having energies near 1 eV primarily from the N_1 position (see Fig. 8) while ca. 1.4 eV is required to cleave the N_3–H bond by electron attachment. In addition, earlier theoretical calculations [19] had shown the N_3–H bond to require more energy to cleave than the N_1–H bond in agreement with [18]. Because we had earlier considered all reasonable (i.e., expected to have low energy barriers) bond cleavages other than the N_3–H bond, it was important that we finalize our series of studies by studying this bond cleavage using the same tools as in our earlier studies.

3.1. Ab initio strategy

Because the thymine π^*-anion is metastable with respect to electron loss, we had to take additional measures to make sure that the energy of the adiabatic state of the anion relative to that of the neutral fragment shown in Fig. 8

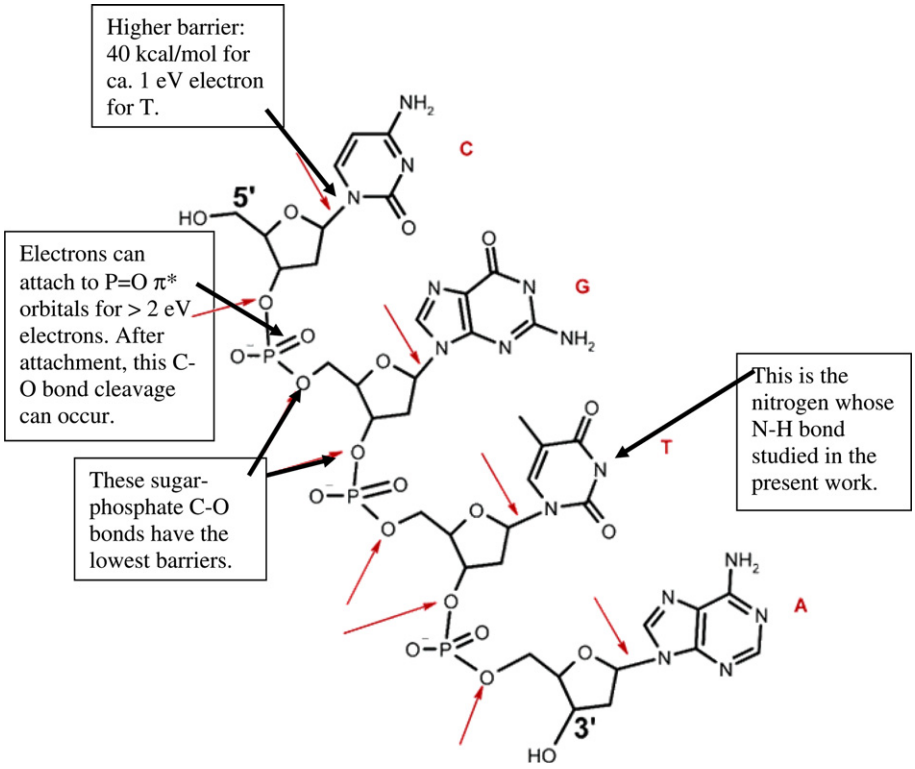

Fig. 7. Structure of DNA (taken from Chart 1 of Ref. [6]) showing the sugar–phosphate C–O bonds having the lowest barriers, the base–sugar N–C bonds having higher barriers, and the N–H bond studied here. Also shown is the site of the P=O π^* orbital to which higher-energy (>2 eV) electrons can attach.

was correct. In particular, we know from Ref. [4] and from our own earlier work at what energy range the low-lying π^* anion states of thymine occur. We thus decided to model attachment of a 1 eV electron to a thymine π^* orbital. To describe attaching an excess electron of energy $E = 1$ eV to the lowest π^*-orbital of thymine, we needed to fine tune our atomic orbital basis set to produce a π^*-attached anion having such an energy. We did so by scaling the exponents of the most diffuse π-type basis functions on the atoms within the thymine ring to generate a π^*-anion that vertically was 1 eV above the neutral. Of course, we also visually inspected the orbital to make sure it indeed was of valence π^* character. Based on our earlier experience, we decided to perform all of our calculations at the unrestricted second-order Møller–Plesset (UMP2) level of theory.

After making sure that our π^*-attached anion was vertically metastable by 1 eV, we then needed to compute the energy of the anion at a range of N_3–H bond lengths to map out the energy profile of the anion as it fragments to release a hydrogen atom. Because the anion is metastable, we could not use conventional quantum chemical methods to construct this energy profile because such calculations would undergo variational collapse [20]. Therefore, we utilized a tool that we have successfully employed in numerous earlier studies of metastable anions. We incremented the nuclear charges of the N_3 nitrogen (from 7 to $7 + \delta q$) and the hydrogen atom (from 1 to $1 + \delta q$) attached to this nitrogen by amounts δq and then evaluated (at the UMP2 level) the energy difference between the neutral thymine and thymine anion (i.e., the artificial "electron binding energy"). If the charge increment δq is large enough, the anion with the artificially enhanced nuclear charges will be rendered stable [21] relative to the neutral (also with enhanced nuclear charges) and thus amenable to conventional quantum chemistry treatment. By computing the electron binding energy vs. δq for values of δq at which the binding energy is positive, we can then extrapolate to $\delta q \rightarrow 0$ to predict the energy of the (metastable) anion relative to the neutral. Of course, we need to perform such charge-stabilization calculations at all values of the N_3–H bond length to generate the desired anion energies.

Finally, we note that all calculations were performed using the Gaussian-03 [22] suite of programs, and the three-dimensional plots of the molecular orbitals were generated with the MOLDEN program [23].

4. Results

From our earlier studies [7–11], we knew that we needed to evaluate the electronic energies of three different electronic states for each value of the N_3–H bond length:

(i) the neutral thymine as it undergoes homolytic cleavage of this N–H bond,
(ii) the anion in which the extra electron is bound to the thymine π^* orbital lying 1 eV above the neutral at the neutral thymine's equilibrium geometry,
(iii) the anion in which the extra electron is bound to the N_3–H σ^* orbital; it is this state that generates the hydrogen atom plus a stable thymine-based anion at large R.

In Fig. 9, we qualitatively illustrate the expected behavior of these three states as functions of the N_3–H bond length.

The spacing between the π^* anion and neutral curves relates to the energy of the metastable state formed when an electron having kinetic energy matching this energy spacing attaches to the neutral thymine. The σ^* anion curve describes how the energy of the anion with two electrons in the N_3–H bonding σ orbital and one in the corresponding anti-bonding σ^* orbital varies. The large-R asymptote of the σ^* anion curve is governed both by the energy needed to homolitically cleave the N_3–H bond and the electron affinity of the N_3-centered radical formed upon bond cleavage. Now, let us discuss how we obtained the actual ab initio neutral, π^* and σ^* anion curves for thymine.

As discussed in Section 3, we needed to use the charge-stabilization method to evaluate the energies of the π^*- and σ^*-anions at N_3–H bond lengths where these states are metastable. In Fig. 10, we show two charge-stabilization plots for the σ^*-attached anion to illustrate and to give the reader some idea of how reliable these extrapolations are.

In Fig. 11, we show the neutral, π^*-attached and σ^*-attached anion energy profiles obtained using the procedures outlined above for thymine.

At N_3–H distances of 1.2 and 1.3 Å, two data points are shown (triangles) for the σ^*-anion to offer the reader some idea of the uncertainties in our extrapolated anion energies.

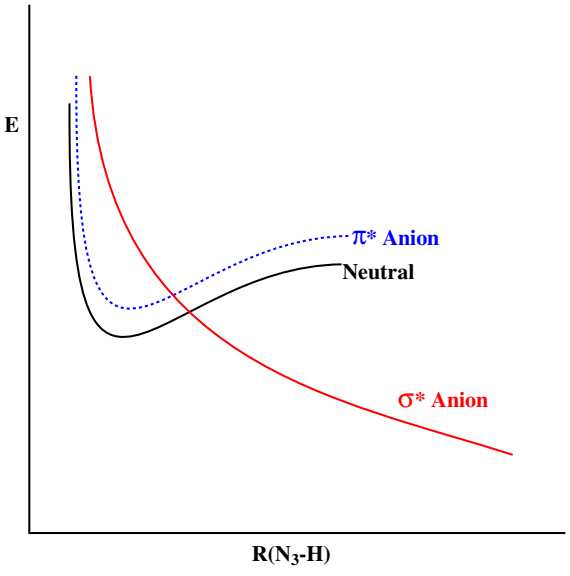

Fig. 9. Expected shapes of the energy profiles for the thymine neutral, π^*-attached anion, and N_3–H σ^*-attached anion as functions of the N_3–H bond length.

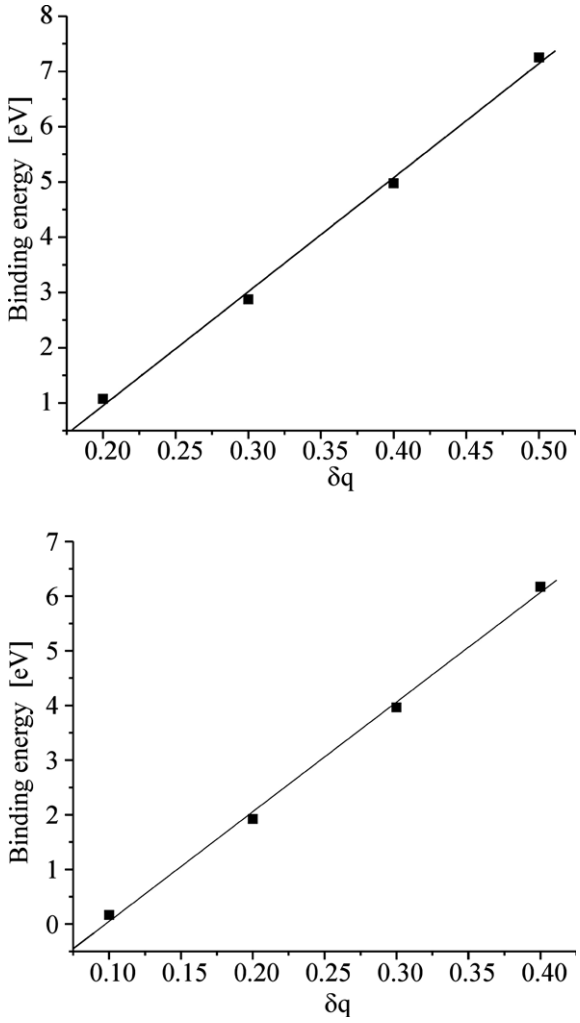

Fig. 10. Charge-stabilization plots of the electron binding energies (eV) as functions of the added nuclear charge (δq) for N_3–H bond lengths of 1.2 Å (top) and 1.3 Å (bottom).

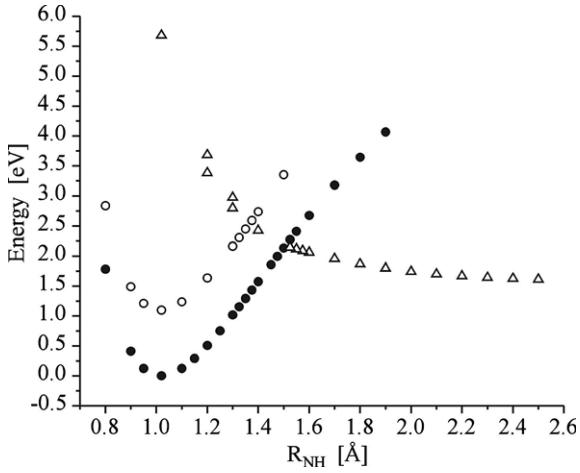

Fig. 11. Energies (eV relative to neutral thymine at its equilibrium geometry) of neutral thymine (filled circles), π^*-attached anion (open circles), and σ^*-attached anion (triangles) as functions of the N_3–H bond length (Å).

The two points at $R = 1.2$ Å were obtained from the charge-stabilization plots extrapolating energies for δq values of 0.2–0.5 (upper triangle) or δq ranging from 0.2 to 0.4 (lower triangle). The two points at $R = 1.3$ Å were obtained by extrapolating energies for δq between 0.1 and 0.4 (upper triangle) or between 0.1 and 0.3 (lower triangle). We expect the data obtained for smaller δq values to be more accurate (because the modification of the electronic Hamiltonian is smallest), so the lower triangles are probably more accurate in each case. However, one can see that considerable error arises in our extrapolated estimates, especially at shorter R-values where the minimum value of δq needed to render stable the σ^* anion is largest.

5. Summary

The primary predictions that we can reach from our results in Fig. 11 are that:

1. When an electron having kinetic energy near 1 eV is attached to a π^* orbital of thymine, there still remains a barrier (where the π^* and σ^* curves cross) of ca. 1.2 eV that must be surmounted before the nascent anion can evolve adiabatically to the σ^* surface and thus cleave the N_3–H bond. This result seems to be in line with the prediction shown in Fig. 1 of Ref. [19].
2. The thermodynamic threshold for N_3–H bond cleavage (the energy difference between the minimum of the neutral and the energy of the anionic fragments) is ca. 1.4 eV.
3. The fact that the experiments [18] show N_3–H bond cleavage to occur at electron energies near 1.4 eV suggests, recalling points 1 and 2 above, that surmounting the 1.2 eV barrier on the thymine anion surface may not be required. Rather, attaching an electron with barely enough energy to place the anion at the energy of its asymptotic fragments may be all that is required. The latter observation, in turn, suggests that tunnelling along the N_3–H bond is involved; otherwise, one would have to surmount the barrier on the anion surface which would require the electron to have 2.2 eV (1.0 eV to access the π^* state and another 1.2 eV to allow the N_3–H bond to surmount the barrier).
4. A refinement of the suggestion offered in point 3 is that thermal excitation of the N_3–H bond (the experiments in Ref. [18] use thymine (T) at 385–400 K) may elongate this bond and thus move the anion upward on the π^*/σ^* surface thus requiring less tunnelling to reach the product $(T–H)^- + H$.
5. Of course, as it pertains to our series of studies concerning SSBs in DNA, it appears that cleavage of the N_3–H bond is not competitive with cleavage of the sugar–phosphate C–O bond where the barrier to be surmounted [24] was ca. 0.5 eV. So, the dominant pathway for SSB formation induced by very low-energy electrons is still predicted to involve C–O bond rupture subsequent to base π^* attachment.

Acknowledgments

J.S. wishes to acknowledge the inspiration that Prof. L. Cederbaum has given the community of chemists who study negative molecular ions over more than 30 years, and he wishes to offer very happy congratulations to Prof. Cederbaum on this special issue. This work was supported by NSF Grants Nos. 9982420 and 0240387 to J.S. Significant computer time provided by the Center for High Performance Computing at the University of Utah and by the Academic Computer Center in Gdansk (TASK) is also gratefully acknowledged.

References

[1] The subject was the subject of a recent popular Science article: G.P. Collins, News Scan, "Fatal Attachments: Extremely low energy electrons can wreck DNA", Scientific American, September issue, pp. 26–28 (2003).
[2] B. Boudaiffa, P. Cloutier, D. Hunting, M.A. Huels, L. Sanche, Science 287 (5458) (2000) 1658.
[3] The DNA samples used in Ref. [2] were quite dry and contained only their structural water molecules. Moreover, their phosphate groups likely had counter cations or protons closely bound to them because the samples did not possess net positive or negative charges. It is very important to keep in mind that all of the experimental and theoretical data discussed in the present paper relate to such neutral samples in which the phosphate groups do not possess negative charges prior to electron attachment.
[4] K. Aflatooni, G.A. Gallup, P.D. Burrow, J. Phys. Chem. A 102 (1998) 6205.
[5] F. Martin, P.D. Burrow, Z. Cai, P. Cloutier, D. Hunting, L. Sanche, Phys. Rev. Lett. 93 (2004) 068101-1-4.
[6] Y. Zheng, P. Cloutier, D.J. Hunting, L. Sanche, J.R. Wagner, J. Am. Chem. Soc. 127 (2005) 16592.
[7] R. Barrios, P. Skurski, J. Simons, J. Phys. Chem. B 106 (2004) 7991.
[8] J. Berdys, I. Anusiewicz, P. Skurski, J. Simons, J. Phys. Chem. A 108 (2004) 2999.
[9] J. Berdys, P. Skurski, J. Simons, J. Phys. Chem. B 108 (2004) 5800.
[10] J. Berdys, I. Anusiewicz, P. Skurski, J. Simons, J. Am. Chem. Soc. 126 (2004) 6441.
[11] I. Anusiewicz, J. Berdys, M. Sobczyk, P. Skurski, J. Simons, J. Phys. Chem. A 108 (2004) 11381.
[12] We terminated with H atoms the –O radical centers and we rendered neutral (by protonation) the negative charge shown in Fig. 1 on the phosphate O atom to simulate the presence of the nearby counter cation (or protonation) that no doubt is present in the dry samples of Ref. [2].
[13] We focused on this particular bond because it was clear to us that its rupture would be thermodynamically favored because of the large (>5 eV) electron affinity of the phosphate unit that is formed upon its cleavage.
[14] X. Li, M.D. Sevilla, L. Sanche, J. Am. Chem. Soc. 125 (2003) 13668.
[15] A.U. Hazi, H.S. Taylor, Phys. Rev. A 1 (1970) 1109.
[16] J. Simons, in: Resonances in Electron-Molecule Scattering, Van Der Waals Complexes, and Reactive Chemical Dynamics, ACS Symposium Series, 1984, pp. 3–16.
[17] We should caution that this conclusion is based upon using SCF-level data on the three-base fragment and MP2-level data on the single-base fragments. It may be that results obtained at the MP2 level for the three-base fragment, which we are now investigating, will alter this conclusion.
[18] S. Ptasinska, S. Denifl, P. Scheier, E. Illenberger, T.D. Märk, Angew. Chem., Int. Ed. 44 (2005) 6941.
[19] X. Li, M.D. Sevilla, L. Sanche, J. Phys. Chem. B 108 (2004) 19013.
[20] Because any simulation begins by carrying out an unrestricted Hartree–Fock (UHF) calculation on the anion, and because such a process is based on the variational principle, it will converge to the lowest-energy state. Unfortunately, this is not the desired π^* resonance state; the lowest state corresponds to the neutral thymine molecule plus an electron as far away as the (finite) atomic orbital basis can describe.
[21] The enhanced nuclear charges differentially stabilize the anion by lowering the valence-range attractive potential that the excess eletron experiences to an extent that the metastable anion state's energy is "puled down" below that of the neutral.
[22] M.J. Frisch, G.W. Trucks, H.B. Schlegel, G.E. Scuseria, M.A. Robb, J.R. Cheeseman, J.A. Montgomery Jr., T. Vreven, K.N. Kudin, J.C. Burant, J.M. Millam, S.S. Iyengar, J. Tomasi, V. Barone, B. Mennucci, M. Cossi, G. Scalmani, N. Rega, G.A. Petersson, H. Nakatsuji, M. Hada, M. Ehara, K. Toyota, R. Fukuda, J. Hasegawa, M. Ishida, T. Nakajima, Y. Honda, O. Kitao, H. Nakai, M. Klene, X. Li, J.E. Knox, H.P. Hratchian, J.B. Cross, C. Adamo, J. Jaramillo, R. Gomperts, R.E. Stratmann, O. Yazyev, A.J. Austin, R. Cammi, C. Pomelli, J.W. Ochterski, P.Y. Ayala, K. Morokuma, G.A. Voth, P. Salvador, J.J. Dannenberg, V.G. Zakrzewski, S. Dapprich, A.D. Daniels, M.C. Strain, O. Farkas, D.K. Malick, A.D. Rabuck, K. Raghavachari, J.B. Foresman, J.V. Ortiz, Q. Cui, A.G. Baboul, S. Clifford, J. Cioslowski, B.B. Stefanov, G. Liu, A. Liashenko, P. Piskorz, I. Komaromi, R.L. Martin, D.J. Fox, T. Keith, M.A. Al-Laham, C.Y. Peng, A. Nanayakkara, M. Challacombe, P.M.W. Gill, B. Johnson, W. Chen, M.W. Wong, C. Gonzalez, J.A. Pople, Gaussian-03, Revision A.1, Gaussian, Inc., Pittsburgh, PA, 2003.
[23] G. Schaftenaar, J.H. Noordik, J. Comput-Aided Mol. Des. 14 (2000) 123.
[24] Unlike the N–H cleavage case, for C–O bond rupture, tunneling is likely not important; instead, the C–O vibration must access and cross the barrier.